

## Photoswitching microscopy with standard fluorophores

S. van de Linde · R. Kasper · M. Heilemann · M. Sauer

Received: 18 August 2008 / Revised version: 2 October 2008 / Published online: 19 October 2008  
© The Author(s) 2008. This article is published with open access at Springerlink.com

**Abstract** We introduce far-field subdiffraction-resolution fluorescence imaging based on photoswitching of individual standard fluorophores in air-saturated solution. Here, photoswitching microscopy relies on the light-induced switching of organic fluorophores (ATTO 655 and ATTO 680) into long-lived metastable dark states and spontaneous repopulation of the fluorescent state. In the presence of low concentrations (2–10 mM) of reducing, thiol-containing compounds such as  $\beta$ -mercaptoethylamine or glutathione, the density of fluorescent molecules can be adjusted to enable multiple localizations of individual fluorophores with an experimental accuracy of  $\sim 20$  nm. The method requires wide-field illumination with only a single laser beam for read-out and photoswitching and provides superresolution fluorescence images of intracellular structures under live cell compatible conditions.

**PACS** 32.50.+d · 61.05.-a · 87.64.M- · 87.80.Nj

### 1 Introduction

Fluorescence microscopes in combination with highly sensitive detection techniques and efficient probes allow a noninvasive 3D study of subcellular structures even in living cells or tissue. However, optical microscopes are subject to the

diffraction barrier of light which imposes an optical resolution limit of approximately 200 nm in the imaging plane. In the recent past, a variety of high-resolution fluorescence methods with different strategies have been introduced that are capable to break the diffraction limit of light [1–8]. These methods can be generalized under the term “photoswitching microscopy,” as they are based on the selective switching of fluorophores between a fluorescent and a non-fluorescent.

Recently, especially wide-field microscopy methods have increasingly emerged that use the fact that a single object can be precisely localized by determining the center of its emission pattern by fitting a two-dimensional Gaussian profile to the individual point spread function (PSF) [9, 10]. That is, photoswitching microscopy approaches such as photoactivation localization microscopy (PALM) [3] or stochastic optical reconstruction microscopy (STORM) [7, 8, 11] and variations thereof [5, 12] attempt to separate the emission of individual fluorescent probes in time. As long as the distance between individual fluorophores enables the unaffected analysis of the different emission spots, i.e., individual fluorophores are spaced further apart than the distance resolved by the microscope ( $> \lambda/2$  on a CCD camera), the standard error of the fitted position is a measure of localization, and it can be made arbitrarily small by collecting more photons and minimizing noise factors. The principle behind these stochastic subdiffraction-resolution fluorescence imaging methods includes repeatedly activating, localizing, and deactivating or bleaching of individual fluorophores to reconstruct a high-resolution fluorescence image of the sample. Ideally, the localization precision of these methods depends only on the number of collected photons  $n$  and on the standard deviation of the PSF ( $\sigma$ ) and can be approximated by  $\sigma/\sqrt{n}$  [9, 13, 14].

S. van de Linde · R. Kasper · M. Heilemann (✉) · M. Sauer  
Applied Laser Physics and Laser Spectroscopy and Bielefeld  
Institute for Biophysics and Nanoscience, Bielefeld University,  
Universitätsstrasse 25, 33615 Bielefeld, Germany  
e-mail: heileman@physik.uni-bielefeld.de  
Fax: +49-521-1062958

M. Sauer  
e-mail: sauer@physik.uni-bielefeld.de

Recently, we demonstrated a new photoswitching microscopy method that relies on the use of organic fluorophores and efficient oxygen removal as well as addition of millimolar concentrations (50–100 mM)  $\beta$ -mercaptoethylamine [7, 11, 15]. Because our approach uses conventional cyanine dyes (Cy5, Alexa 647) for cellular staining and is not relying on the proximity of two fluorophores, both being attached to an antibody in a specific ratio and distance as is required for STORM [8, 16], it is marked as “direct,” *d*STORM. Essentially, the strength of *d*STORM lies in its compatibility with any fluorescence method that enables the labeling of target molecules with a reversible photoswitchable fluorophore [15], e.g., via immunocytochemistry using antibodies or Fab-fragments, or through labeling of peptides or nucleic acids, or direct labeling of biomolecules or any other target molecule [7]. The fluorescence emission of single carbocyanine molecules is read out with excitation at 647 nm until the fluorophore enters a nonfluorescent dark state. Through irradiation in the blue/green, e.g., at 514 nm, the fluorophore can be switched back to the fluorescent state. This transition is reversible and was demonstrated to occur highly reliably up to hundred times per single fluorophore [15]. During each fluorescence cycle, typically a few hundred photons are emitted before the fluorophore enters again the dark state.

Importantly, we could recently demonstrate that photoswitching microscopy is not restricted to subdiffraction-resolution fluorescence imaging but can be used likewise efficiently for molecular quantification, i.e., the determination of absolute numbers and densities of proteins localized in specific subcellular compartments [11]. Since all methods exploiting control of fluorophore emission to increase optical resolution or to gain quantitative information critically depend on the availability of efficient photoswitches, they are highly demanded [6, 17]. The ideal photoswitch is characterized by two spectrally well-separated thermally stable states, a high switching reliability and low fatigue which determines the number of switching cycles the molecules can survive, a high fluorescence quantum yield in the fluorescent state, a high photostability, and tunable switching rates.

The current drawbacks of photoswitching microscopy are the limited accessibility of efficient photoactivatable or photoswitchable fluorophores in different colors and the necessity of an adequate second laser for activation of the fluorophore, as well as biological incompatible environmental requirements such as oxygen removal [3, 7, 8, 18–23]. Here, we demonstrate for the first time that long-lived dark states of ordinary fluorophores such as ATTO 655 and ATTO 680 can be used advantageously for subdiffraction-resolution fluorescence imaging in air-saturated solution using wide-field illumination with a single laser beam at 647 nm with moderate power (20–40 mW). Through the addition of millimolar concentrations (2–10 mM) of  $\beta$ -mercaptoethylamine

(MEA) or glutathione presumably radical anions are formed with lifetimes of several tens to hundreds of milliseconds. Thus, the density of fluorescent molecules can be confined temporally to enable photoswitching microscopy, i.e., the repeated localization of individual spontaneously activated fluorophores. Since reducing thiol-containing compounds such as glutathione are also present in living cells in the lower millimolar range, our results raise hope that conventional standard fluorophores can be used for photoswitching microscopy with superresolution under biologically compatible conditions.

## 2 Materials and methods

**Cell culture and immunocytochemistry:** African green monkey kidney COS-7 cells were plated in LabTek 8-well chambered coverglass (Nunc). After 12 to 24 hours, the cells were fixed using 3.7% paraformaldehyde in phosphate-buffered saline (PBS) for 10 min. The fixed cells were washed five times with PBS, permeabilized (PBS containing 0.5% v/v Triton X-100) for 10 min, and treated with blocking buffer (PBS containing 5% w/v normal goat serum (NGS; Sigma) for 30 min). Microtubules were stained with mouse monoclonal anti- $\beta$ -tubulin antibodies (clone: TUB 2.1, Sigma) for 60 min. Subsequently, cells were stained for 60 min with ATTO 655 (Atto-Tec GmbH; AD 655-3) labeled goat anti-mouse F(ab')<sub>2</sub> fragments (Invitrogen, M35000). Three washing steps using PBS containing 0.1% v/v Tween 20 were performed after each staining step. Labeled F(ab')<sub>2</sub> fragments were purified on an NAP 5 column (Sephadex G-25 DNA Grade, GE Healthcare), and the labeling ratio of F(ab')<sub>2</sub> fragments with ATTO 655 was determined to  $\sim$ 1.8.

**Direct Stochastic Optical Reconstruction Microscopy (*d*STORM):** Fluorescence imaging was performed on an Olympus IX-71 applying an objective-type total internal reflection fluorescence (TIRF) configuration equipped with an oil-immersion objective (PlanApo 60 $\times$ , NA 1.45, Olympus) and was described earlier [7, 11]. The 647 nm laser beam of an argon-krypton laser (Innova 70C, Coherent) was selected by an acousto-optical transmission filter (AOTF) and coupled into the microscope objective by a polychromic beam-splitter (532/647, AHF Analysentechnik). Fluorescence light was spectrally filtered with two filters (ET 700/75 and HQ665LP, AHF Analysentechnik) and imaged on an EMCCD camera (Andor Ixon+DV897DCS-BV). Additional lenses were used to achieve a final imaging magnification of 225, i.e., a pixel size of 70 nm. Single-molecule photoswitching of ATTO 655 and ATTO 680 was performed in PBS, pH 7.4, containing 2–10 mM  $\beta$ -mercaptoethylamine (MEA) or glutathione. Photoswitching microscopy was performed with a laser power of 22–40 mW. Typically, 8000–16000 images were recorded at a frame rate of 10–100 Hz

corresponding to measurement times of 80 seconds to 26.7 minutes. The accuracy of localization depends on the number of photons detected,  $N$ , and the standard deviation of the PSF,  $\sigma$ , and can be approximated as  $\sigma/\sqrt{N}$  [13]. Here, typically 500 to 1000 photons were typically detected for a single ATTO 655 or ATTO 680 fluorophore in its on-state. With a standard deviation of the PSF of  $\sim 250$  nm for the emission of ATTO 655 (absorption and emission maxima are centered at  $\sim 660$  and  $680$  nm, respectively [24]), we can expect a localization precision down to  $\sim 10$  nm. Under these imaging conditions, the fluorophores remain in the active state for several frames after spontaneous activation resulting in several thousand photons detected per fluorophore and switching cycle. *d*STORM images were generated as described previously [7, 11]. Briefly, individual spots were identified in each image frame applying an intensity threshold and were fit to a Gaussian function to determine their centre of mass. All coordinates of single molecules were used to reconstruct the *d*STORM image, and a subpixel size of  $7 \times 7$  nm<sup>2</sup> was applied.

### 3 Results and discussion

Since photoswitching microscopy intrinsically only requires switching of a fluorophore between a fluorescent and a non-fluorescent state, any dark state such as the triplet state which is naturally present in virtually all fluorophores can be used. This finding has been used in ground-state depletion (GSD) microscopy to achieve subdiffraction-resolution fluorescence imaging in combination with a depletion beam featuring a local zero in the focus [25]. Thus, the light-driven occupation of the metastable triplet state might provide a general platform onto which to base the development of an alternative photoswitching microscopy method with conventional fluorophores. Upon excitation a fluorophore enters the triplet state,  $T_1$ , dependent on its intersystem crossing yield. After a certain time, the triplet state lifetime, it returns back spontaneously to the singlet ground-state,  $S_0$ , where it can be repeatedly cycled between  $S_0$  and the first excited singlet state,  $S_1$ , and emit fluorescence photons used to precisely localize its position.

However, photoswitching microscopy requires the majority of fluorophores to reside in the dark state, i.e., the dark state should exhibit a lifetime that is substantially longer than the typical time the fluorophore stays in its active, fluorescent form. Unfortunately, the triplet state lifetimes of standard fluorophores such as rhodamine, oxazine, and carbocyanine dyes are short and vary between less than 1  $\mu$ s up to a few hundred  $\mu$ s in air-saturated solution, with intersystem crossing rates  $k_{isc}$  from  $4.2 \times 10^5$  to  $2.8 \times 10^7$  s<sup>-1</sup> [26–31] corresponding to relatively low quantum yields,  $\Phi_{isc} < 0.1\%$ . In order to use the triplet state

for photoswitching microscopy, relatively high excitation intensities are required to efficiently populate the triplet state. In addition, the triplet state lifetime (off time) should be considerably longer than the on time, i.e., triplet state lifetimes of several milliseconds, ideally tens of milliseconds, are required to ensure the spatially separated detection and localization of individual fluorophores.

The on time, i.e., the time the fluorophore spends in the singlet manifold, can be controlled by the excitation intensity and can thus principally be reduced to a few milliseconds. On the other hand, the much shorter-lived triplet state lifetime can be prolonged upon oxygen removal because oxygen is known as very potent triplet quencher. For example, in vacuum, triplet state lifetimes of 4–100 ms have been measured with a triplet yield of 0.04% for single DiIC12 molecules (a carbocyanine derivative) [32]. Similar values were measured for fluorophores immobilized in thin polymer films such as PVA with low oxygen permeability [33, 34]. Alternatively, one can remove oxygen from aqueous solutions using efficient enzymatic scavenger systems as used in the STORM and *d*STORM methods [7, 8, 11, 15, 35, 36]. Very recently, these strategies were successfully implemented to introduce a new photoswitching microscopy method termed ground state depletion microscopy followed by individual molecule return (GSDIM) [37].

On the other hand, triplet state lifetimes are long enough to serve as origin for reactions with additives to produce alternative long-lived dark states such as radical ion states. These findings form the basis for the recently introduced reducing and oxidizing system (ROXS) that minimizes blinking and substantially increases the photostability of various fluorophores [38]. ROXS uses electron transfer reactions to control the off times of fluorophores. The idea behind is that in the absence of oxygen the long-lived triplet states can be depopulated via electron transfer reactions to form radical ions, i.e., either radical anions or cations dependent on the additive, which possess a considerably longer lifetime than the triplet state. This elegant method offers the possibility to engineer the lifetime of the dark state of principally any fluorophore by addition of different concentrations of a triplet quencher (a reducing or oxidizing reagent) and thus might enable the use of a variety of fluorophores for photoswitching microscopy.

In addition, such strategies benefit from the fact that only a single laser wavelength is required because the fluorescent state is repopulated spontaneously from the nonfluorescent dark state. The drawback of such strategies is, however, the control of the density of fluorophores residing in the singlet manifold, i.e., in their fluorescent states, especially for densely labeled samples. Just as a reminder, photoswitching microscopy requires a density of less than one fluorescent molecule present in the diffraction area at any time. This is

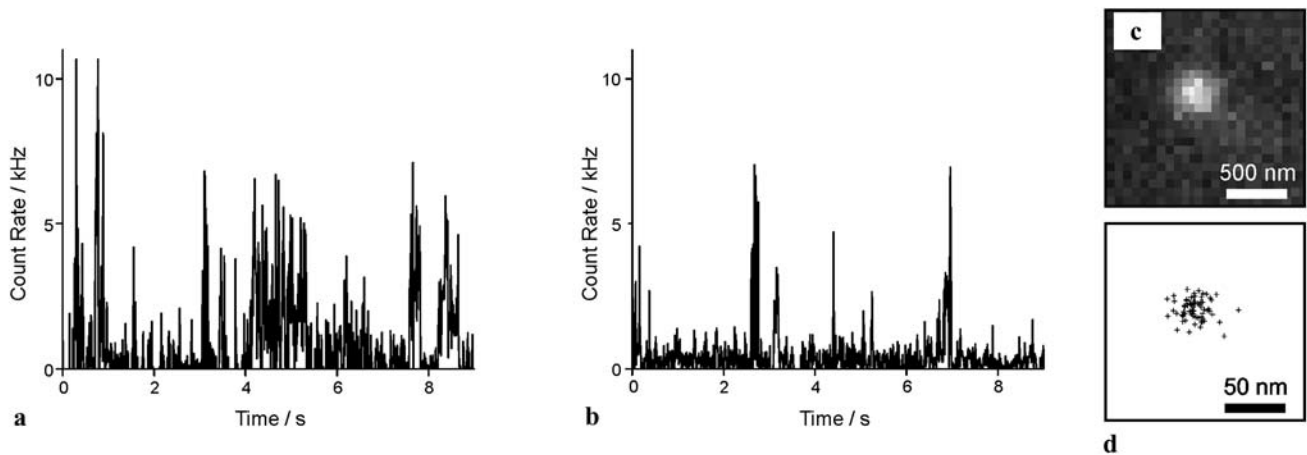


**Fig. 1** Fluorescence time traces of a single ATTO 655 labeled goat anti-mouse  $F(ab')_2$  fragment adsorbed non-specifically on a glass coverslide recorded under continuous illumination with a frame rate of 10 Hz in the presence of 2 mM (a) and 10 mM MEA (b). (c) Image (PSF) of a single ATTO 655 labeled  $F(ab')_2$  fragment. (d) Repetitive

localizations (represented as *crosses*) of a single immobilized ATTO 655 labeled  $F(ab')_2$  fragment switching between its fluorescent and dark state. Measurements were performed in PBS, pH 7.4 at a laser power of 24 mW at 647 nm using TIRF microscopy

easily controllable in standard photoswitching microscopy approaches because the density of fluorescent molecules can be adjusted by the illumination power of the activation laser. That is, the sample can be irradiated with high intensity to turn the majority of photoswitches into their nonfluorescent states and recover only a subpopulation determined by the activation laser power. When long-lived triplet or radical ion states are used as nonfluorescent states very high excitation powers have to be used to drive the majority of fluorophores into their triplet states prior to imaging to ensure the desired density of fluorescent molecules. This has the drawback that some fluorophores will be irreversibly photobleached.

In addition, the accessibility of a variety of fluorophores in different wavelength ranges through tuning of their off-states by external additives and oxygen removal or immobilization in polymers prevents applications in live cell experiments. Interestingly, some oxazine fluorophores show very long off-times with lifetimes of up to 100 ms even under air-saturated conditions with relatively low yields in the order of  $10^{-5}$  [31, 39]. To further increase the yield of these long-lived off states  $\beta$ -mercaptoethylamine (MEA), a reducing thiol-containing compound can be added in the lower millimolar concentration range (Fig. 1a). Although MEA at lower millimolar concentrations shows only weak quenching of the  $S_1$  state of the fluorophore (here ATTO 655 a fluorophore with photophysical characteristics similar to those of the oxazine derivative MR121 [24]), it is very likely that it promotes the formation of long-lived radical anion states generated via reduction of the  $T_1$  state [38] even in the presence of oxygen. Thus, the lifetime of the off state can be adjusted by the MEA concentration (compare Figs. 1a and b). On the other hand, the lifetime of the on state is mainly controlled by the excitation power as expected for a pho-

toinduced process and as was found to vary between tens to hundreds of milliseconds. Here it has to be pointed out that a detailed analysis of on and off states is complicated by the fact that the Fab fragments used in our experiments exhibit an average degree of labeling of  $\sim 1.8$ , i.e., most antibodies carry two fluorophores. To perform wide-field photoswitching microscopy with subdiffraction-resolution, only a single laser source with moderate excitation power is required. Among several other fluorophores tested ATTO 680, a structurally very similar dye with slightly red-shifted spectroscopic properties (ATTO 655 and ATTO 680 exhibit absorption/emission maxima in aqueous buffer at 663/684 nm and 680/700 nm, respectively) shows identical photoswitching performance. We varied the concentration of MEA in the range of 2–100 mM and found concentrations of  $\leq 10$  mM to be best suited for photoswitching microscopy with ATTO 655 and ATTO 680 (Figs. 1a and b). At higher MEA concentrations, fluorescence quenching of the singlet state starts to decrease the photon yield.

The finding that some fluorophores such as ATTO 655 and ATTO 680 show similar photoswitching performance as reversibly photoswitchable carbocyanine dyes [15] upon continuous illumination with a single red laser beam of moderate power in the presence of oxygen motivated us to use these fluorophores for subdiffraction-resolution fluorescence imaging, i.e., *d*STORM. Fluorescence images of samples were generated by wide-field fluorescence microscopy upon excitation at 647 nm. The resulting PSFs of individual spontaneously activated fluorophores (Fig. 1c) were analyzed by fitting a Gaussian function to localize their positions with high precision. After thousands of position determinations (localizations), the superresolution image was reconstructed. As can be seen in Figs. 1a and b, typically 500

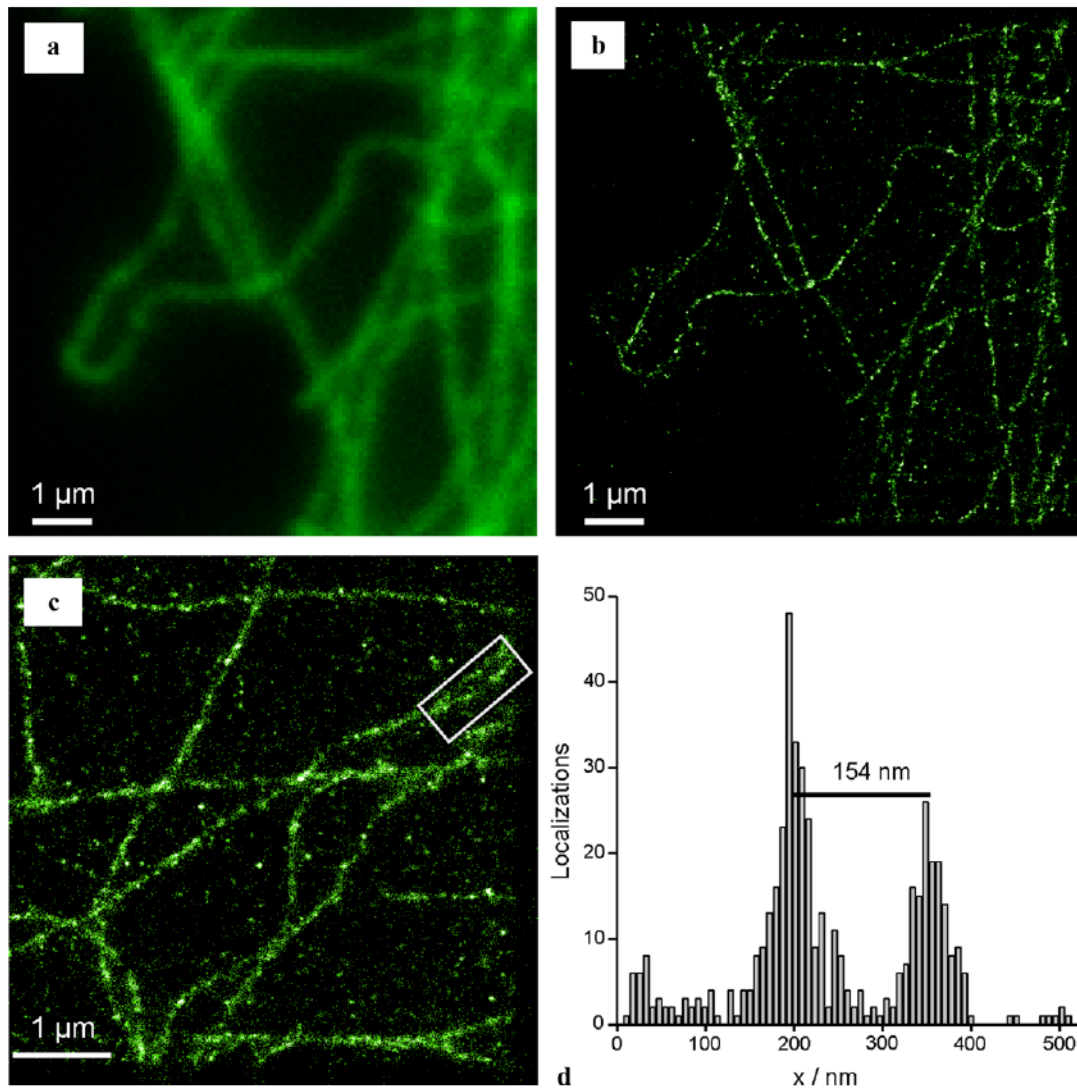


**Fig. 2** (a) Conventional immuno-fluorescence images of microtubules in COS-7 cells labeled with a primary antibody and ATTO 655 labeled goat anti-mouse F(ab')<sub>2</sub> fragments and corresponding *d*STORM image (b) measured with an image acquisition rate of 10 Hz. (c) *d*STORM image recorded with 10 Hz frame rate and (d) cross-sectional profile

of adjacent microtubule filaments arranged 154 nm apart in the cell (white rectangle in (c)). Measurements were performed in PBS, pH 7.4, containing 10 mM MEA at a laser power of 24 mW at 647 nm using TIRF microscopy

to 1000 fluorescence photons can be detected for single ATTO 655 fluorophores suggesting an optimal localization precision  $\sim 10$  nm [9]. However, the cluster of localizations shown in Fig. 1d resulting from repetitive localizations of a single immobile ATTO 655 labeled F(ab')<sub>2</sub> fragment demonstrates that a real experimental optical resolution of  $\sim 20$  nm can be achieved for fluorescence imaging with standard fluorophores under air-saturated conditions without mechanical stabilization of the setup.

To demonstrate the potential of the new method for subdiffraction-resolution fluorescence imaging of cellular structures, we used fixed COS-7 cells and stained the microtubular network applying immunocytochemistry and an-

tibody fragments labeled with ATTO 655. Figure 2a shows a conventional fluorescence image using an excitation wavelength of 647 nm in the presence of 10 mM MEA. In a next step, we increased the laser intensity to 24 mW, to turn the majority of fluorophores into their long-lived dark states and reconstructed high-resolution images from the spontaneously activated fluorophores. As can be easily seen in Figs. 2b and c, the *d*STORM images show superior resolution as compared to conventional wide-field images of the microtubule network. The improvement in spatial resolution achieved with *d*STORM is demonstrated with single microtubule filaments (Figs. 2c and d). As can be seen in Fig. 3, our new method is not restricted to the use of  $\beta$ -mercaptoethylamine but likewise works in the presence of

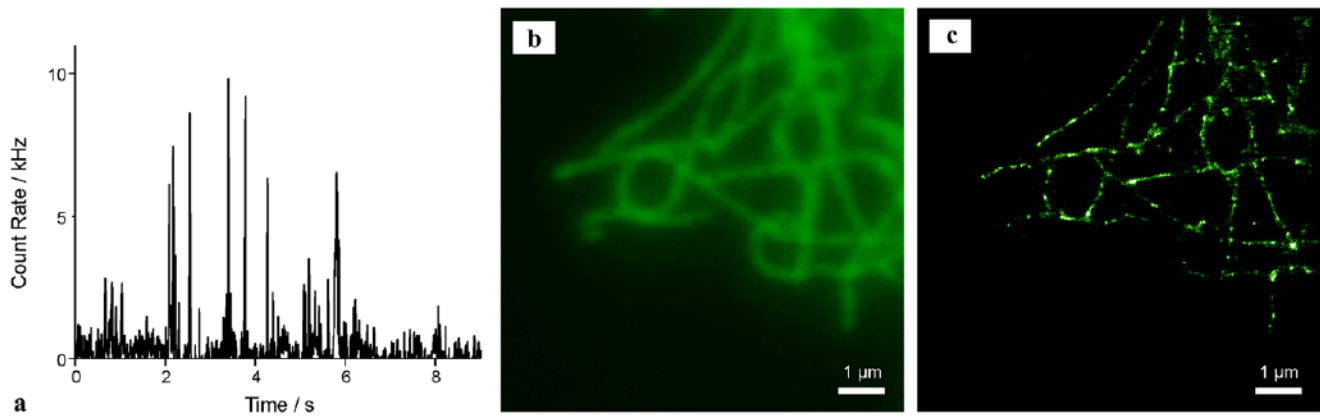


**Fig. 3** (a) Fluorescence time trace of a single ATTO 655 labeled goat anti-mouse F(ab')<sub>2</sub> fragment adsorbed non-specifically on a glass coverslide recorded under continuous illumination with a frame rate of 10 Hz in the presence of 10 mM glutathione. (b) Conventional immunofluorescence image of microtubules in COS-7 cells labeled with a primary antibody and ATTO 655 labeled goat anti-mouse F(ab')<sub>2</sub> frag-

ments and (c) corresponding dSTORM image reconstructed from 8000 images taken with an image acquisition rate of 100 Hz, resulting in a total acquisition time of 80 seconds. Measurements were performed in PBS, pH 7.4, containing 10 mM glutathione at a laser power of 40 mW at 647 nm using TIRF microscopy

biologically compatible compounds such as glutathione, a major intracellular non-protein thiol compound with reducing properties. In addition, considerably shorter measurement times with frame rates of 100 Hz can be used (Fig. 3c).

#### 4 Conclusion

In conclusion, we have demonstrated far-field fluorescence photoswitching microscopy with  $\sim 20$  nm effective resolution using a single continuous laser source and moderate excitation powers. Even more important, we introduced novel photoswitches that do not require oxygen removal, but only the addition of a reducing thiol-containing compound in the lower millimolar range. These findings further suggest the compatibility of these photoswitches with live cell imaging, as it is known that cells, besides many thiol-containing proteins, contain glutathione in the lower millimolar concentration range (i.e., up to 10 mM). The tripeptide glutathione is a major intracellular non-protein thiol compound with reducing properties and is essential for the optimum activity of some enzymes and other cellular macromolecules as well as for detoxication [40–42]. As can be seen in Fig. 3, the presence of 10 mM glutathione enables subdiffraction-resolution fluorescence microscopy in the presence of oxygen even with frame rates of 100 Hz. Hence, a superresolution image can be recorded in only 80 seconds (Fig. 3c). Therefore, we believe that our new method might pave the way towards in vivo superresolution fluorescence imaging microscopy. The relatively simple experimental procedure of photoswitching of conventional fluorophores with only one excitation laser by exploiting a transition into a long-lived triplet or radical state raises hope that also other fluorophores in the green

wavelength range can be used without addition of any additives or removal of oxygen under intracellular conditions. Although these strategies might have limitations with respect to the adjustment of the optimal density of fluorescent molecules for subdiffraction-resolution fluorescence imaging, one should consider that photoswitches are likewise useful for molecular quantification experiments where the number of fluorophores is controlled by the protein density [11].

**Acknowledgements** The authors would like to thank Dr. Gerd Wiebusch for technical assistance. This work was supported by the Biophotonics and the Systems Biology Initiative (FORSSYS) of the German Ministry of Research and Education (BMBF, grants 13N9234 and 0315262).

**Open Access** This article is distributed under the terms of the Creative Commons Attribution Noncommercial License which permits any noncommercial use, distribution, and reproduction in any medium, provided the original author(s) and source are credited.

#### References

1. S.W. Hell, J. Wichmann, *Opt. Lett.* **19**, 780 (1994)
2. M.G. Gustafsson, D.A. Agard, J.W. Sedat, *J. Microsc.* **195**, 10 (1999)
3. E. Betzig, G.H. Patterson, R. Sougrat, O.W. Lindwasser, S. Olenych, J.S. Bonifacino, M.W. Davidson, J. Lippincott-Schwartz, H.F. Hess, *Science (New York)* **313**, 1642 (2006)
4. H. Bock, C. Geisler, C.A. Wurm, C. Von Middendorff, S. Jakobs, A. Schonle, A. Egner, S.W. Hell, C. Eggeling, *Appl. Phys. B Lasers Opt.* **88**, 161 (2007)
5. P. Dedecker, J. Hotta, C. Flors, M. Sliwa, H. Uji-i, M.B. Roefsaers, R. Ando, H. Mizuno, A. Miyawaki, J. Hofkens, *J. Am. Chem. Soc.* **129**, 16132 (2007)
6. S.W. Hell, *Science (New York)* **316**, 1153 (2007)

7. M. Heilemann, S. van de Linde, M. Schuettpelz, R. Kasper, B. Seefeldt, A. Mukherjee, P. Tinnefeld, M. Sauer, *Angew. Chem.* **47**, 6172 (2008)
8. B. Huang, W. Wang, M. Bates, X. Zhuang, *Science (New York)* **319**, 810 (2008)
9. M.K. Cheezum, W.F. Walker, W.H. Guilford, *Biophys. J.* **81**, 2378 (2001)
10. A. Yildiz, J.N. Forkey, S.A. McKinney, T. Ha, Y.E. Goldman, P.R. Selvin, *Science (New York)* **300**, 2061 (2003)
11. S. van de Linde, M. Sauer, M. Heilemann, *J. Struct. Biol.* (2008). doi:10.1016/j.jsb.2008.08.002
12. J. Enderlein, *Appl. Phys. Lett.* **87**, 094105 (2005)
13. R.E. Thompson, D.R. Larson, W.W. Webb, *Biophys. J.* **82**, 2775 (2002)
14. S. Ram, E.S. Ward, R.J. Ober, *Proc. Nat. Acad. Sci. US Am.* **103**, 4457 (2006)
15. M. Heilemann, E. Margeat, R. Kasper, M. Sauer, P. Tinnefeld, *J. Am. Chem. Soc.* **127**, 3801 (2005)
16. M.J. Rust, M. Bates, X. Zhuang, *Nat. Methods* **3**, 793 (2006)
17. M. Sauer, *Proc. Nat. Acad. Sci. US Am.* **102**, 9433 (2005)
18. S.T. Hess, T.P. Girirajan, M.D. Mason, *Biophys. J.* **91**, 4258 (2006)
19. A. Egner, C. Geisler, C. von Middendorff, H. Bock, D. Wenzel, R. Medda, M. Andresen, A.C. Stiel, S. Jakobs, C. Eggeling, A. Schonle, S.W. Hell, *Biophys. J.* **93**, 3285 (2007)
20. C. Flors, J. Hotta, H. Uji-i, P. Dedecker, R. Ando, H. Mizuno, A. Miyawaki, J. Hofkens, *J. Am. Chem. Soc.* **129**, 13970 (2007)
21. J. Fölling, V. Belov, R. Kunetsky, R. Medda, A. Schonle, A. Egner, C. Eggeling, M. Bossi, S.W. Hell, *Angew. Chem.* **46**, 6266 (2007)
22. M.F. Juetten, T.J. Gould, M.D. Lessard, M.J. Mlodzianoski, B.S. Nagpure, B.T. Bennett, S.T. Hess, J. Bewersdorf, *Nat. Methods* **5**, 527 (2008)
23. H. Shroff, C.G. Galbraith, J.A. Galbraith, E. Betzig, *Nat. Methods* **5**, 417 (2008)
24. V. Buschmann, K.D. Weston, M. Sauer, *Bioconjug. Chem.* **14**, 195 (2003)
25. S. Bretschneider, C. Eggeling, S.W. Hell, *Phys. Rev. Lett.* **98**, 218103 (2007)
26. K.H. Drexhage, *Structure and Properties of Laser Dyes*, vol. 1 (Springer, Berlin, 1973)
27. M.M. Asimov, V.N. Gavrilenko, A.N. Rubinov, *J. Lumin.* **46**, 243 (1990)
28. R. Menzel, E. Thiel, *Chem. Phys. Lett.* **291**, 237 (1998)
29. R. Menzel, R. Bornemann, E. Thiel, *Phys. Chem. Chem. Phys.* **1**, 2435 (1999)
30. J. Widengren, P. Schwille, *J. Phys. Chem. A* **104**, 6416 (2000)
31. P. Tinnefeld, D.P. Herten, M. Sauer, *J. Phys. Chem. A* **105**, 7989 (2001)
32. K.D. Weston, P.J. Carson, J.A. DeAro, S.K. Buratto, *Chem. Phys. Lett.* **308**, 58 (1999)
33. D.S. English, A. Furube, P.F. Barbara, *Chem. Phys. Lett.* **324**, 15 (2000)
34. P. Tinnefeld, V. Buschmann, K.D. Weston, M. Sauer, *J. Phys. Chem. A* **107**, 323 (2003)
35. Y. Harada, K. Sakurada, T. Aoki, D.D. Thomas, T. Yanagida, *J. Mol. Biol.* **216**, 49 (1990)
36. T. Ha, I. Rasnik, W. Cheng, H.P. Babcock, G.H. Gauss, T.M. Lohman, S. Chu, *Nature* **419**, 638 (2002)
37. J. Fölling, M. Bossi, H. Bock, R. Medda, C.A. Wurm, B. Hein, S. Jakobs, C. Eggeling, S.W. Hell, *Nat. Methods* (2008). doi:10.1038/nmeth.1257
38. J. Vogelsang, R. Kasper, C. Steinhauer, B. Person, M. Heilemann, M. Sauer, P. Tinnefeld, *Angew. Chem.* **47**, 5465 (2008)
39. P. Tinnefeld, V. Buschmann, D.P. Herten, K.-T. Han, M. Sauer, *Single Mol.* **1**, 215 (2000)
40. C.W. Parker, C.M. Fischman, H.J. Wedner, *Proc. Nat. Acad. Sci. US Am.* **77**, 6870 (1980)
41. J. Vina, J.M. Estrela, C. Guerri, F.J. Romero, *Biochem. J.* **188**, 549 (1980)
42. H. Sies, *Free Radic. Biol. Med.* **27**, 916 (1999)